Finite Element Analysis of all Modes in Cavities with Circular Symmetry

J. BRIAN DAVIES, MEMBER, IEEE, F. ANIBAL FERNANDEZ, AND GLAFKOS Y. PHILIPPOU, MEMBER, IEEE

Abstract—**A field analysis is presented of all modes in a hollow, conducting cavity with rotational symmetry about an axis. Cavities can be periodic along this axis, and the unit (or single) cell can be of arbitrary longitudinal section, with inhomogeneous dielectric loading. Modes of any angular dependence of arbitrary phase-shift per unit cell are analyzed. The finite element method is applied in the longitudinal plane, and uses a specially developed sparse matrix scheme.**

I. Introduction

A COMMON TYPE of electromagnetic cavity consists of a conducting surface of revolution about an axis. Sometimes, there is a single such cavity, but often a longitudinally periodic structure of such cavities is used, as in Fig. 1, and both types are considered in this work.

Because of the large investment in particle accelerators, with their applications to medicine and physics, the most serious studies of these cavities have come from this field. For more than three decades the linear accelerator type of cavity has been studied [1]–[3], with attention almost exclusively paid to the angular-independent TM_{0m} (accelerating) modes. Good cavity design depends on a field analysis of these 'accelerating' modes, to give dispersion, series impedance, etc., and the latest computer programs [4], [5] deal with such analysis, giving the dispersion characteristics and fields of a single hollow cavity of arbitrary longitudinal section.

The chief omission from previous cavity theories has been the failure to consider angular dependent modes. Because of their relevance to 'pulse-shortening' [6] and to particle separators [7], angular-dependent modes (which have angular dependence $\cos(n\theta)$ or $\sin(n\theta)$, and include all three components of $\boldsymbol{E}$ and $\boldsymbol{H}$) have been studied for the special 'circular iris-loaded waveguide' geometry [6], [7].

The work now to be described is an advance on existing theory in being able to analyze: i) angular dependent modes (E/H_{nm} or H/E_{nm}) as well as angular independent modes (TM_{0m} or TE_{0m}) for hollow cavities of arbitrarily shaped longitudinal section (which may be singly- or multiply-connected); ii) a periodic (along the z-axis) structure of such cavities, where operation is at an arbitrary phase shift per 'unit cell'; and iii) an inhomogeneous dielectric loading of the above cavities, where the structure remains cylindrically symmetrical.

Manuscript received April 29, 1982; revised July 8, 1982.

J. B. Davies is with the Department of Electrical Engineering, University College, Torrington Place, London WC1E 7JE, England.

F. A. Fernandez is with the Departamento de Ingenieria Electrica, Universidad de Chile, Av. Tupper 2007, Casilla 5037, Santiago, Chile.

G. Y. Philippou is with ERA Technology Limited, Cleeve Road, Leatherhead, Surrey, KT22 7SA, England.

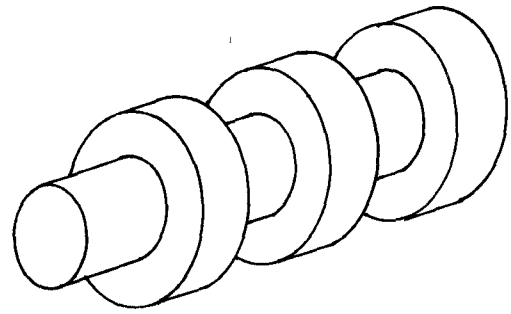

Fig. 1. Periodic hollow cavity.

II. Theory

The microwave structure under study is assumed to be periodic and infinite in length, composed of identical and equally spaced cells of arbitrary longitudinal section, and to be rotationally symmetric with respect to the axis, as shown in Fig. 1.

Application of Floquet's theorem [8] allows us to consider the fields in only one cell. The fields in any other cell distance pL away from the basic cell are just $\exp(-j\beta_0 pL)$ times those in the basic cell. This imposes on the fields a restriction additional to the usual conducting boundary conditions. The fields in the section S_2 at $z = L$ are therefore $\exp(-j\beta_0 L)$ times the fields in S_1 at $z = 0$, where L is the length of the cell as in Fig. 2.

We will consider fields with time dependence $\exp(j\omega t)$ and, as the structure is rotationally symmetric, the angular dependence will be taken as $\exp(-jn\theta)$ where n is an integer. The problem is to find the fields that satisfy Maxwell's equations throughout the unit cell, including the usual conducting boundary conditions on the walls, and that also satisfy the above mentioned periodicity condition. In practice, what is wanted is the value of the angular frequency ω and the corresponding field distribution over the unit cell which satisfies the conditions for a specified value of $\beta_0 L$, the phase shift per unit cell.

Transverse electric and transverse magnetic modes can exist separately in this corrugated waveguide only if they are angularly independent. Angular dependent modes can only exist as hybrid modes, with a combination of the

0018-9480/82/1100-1975$00.75 ©1982 IEEE

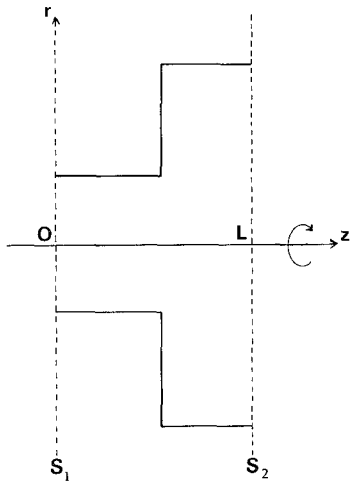

Fig. 2. Longitudinal section of a unit cell (single cavity).

associated TE and TM fields, and these were included in the earlier studies of iris-loaded periodic guides [6].

A. Variational and Finite Element Formulation

The above problem will now be solved using a variational and finite element approach. A variational principle is formulated in terms of the three-component magnetic field, and stationary values are sought by the Rayleigh–Ritz and finite element methods.

For the simple TM_0 angular independent modes, the choice of a scalar variational expression is immediate [4], but for hybrid modes the choice is more difficult. A variational form can be in terms of: i) the longitudinal components only of E and H; ii) the transverse components of $\boldsymbol{H}$; iii) the transverse components of $\boldsymbol{E}$; iv) the complete vector field $\boldsymbol{H}$; v) the complete $\boldsymbol{E}$, or vi) the complete fields $\boldsymbol{H}$ and $\boldsymbol{E}$. Methods i)–iii) are the most economical, in requiring only two scalar components of field, but the process of economizing introduces a disparity between the six field components that involves numerical singularities and spurious solutions. For instance, modes with phase velocities near the speed of light (which are clearly important for particle accelerators or separators) have a singularity in their transverse fields as functions of radial wavenumber, a singularity that is inevitable with the TM and the TE formulation of method i) [6], [7]. Method iv), with the complete $\boldsymbol{H}$ vector field formulation, introduces no disparity between the three components, involves a field that is spatially continuous and bounded even in the presence of the discontinuously inhomogeneous dielectric, and immediately gives correct 'natural boundary conditions' at the conducting boundaries. We therefore use as variational formulation

$$\omega^2 = \frac{\int (\nabla \times \boldsymbol{H})^* \epsilon^{-1} (\nabla \times \boldsymbol{H})\, dv}{\int \boldsymbol{H}^* \mu \boldsymbol{H}\, dv} \tag{1}$$

For trial fields $\boldsymbol{H}(r, z)$ defined over the unit cell (Fig. 2) such that

$$\boldsymbol{H}(r, z) = \boldsymbol{H}(r, z + L) \exp(j\beta_0 L) \tag{2}$$

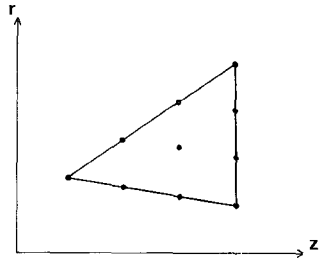

Fig. 3. Nodal arrangement for triangular element with third-degree polynomial.

it has been shown [9], [10] that (1) is stationary, with

$$\nabla \times (\epsilon^{-1} \nabla \times \boldsymbol{H}) - \omega^2 \mu \boldsymbol{H} = 0 \tag{3}$$

as the associated Euler equation and

$$\boldsymbol{n} \times (\epsilon^{-1} \nabla \times \boldsymbol{H}) = 0 \tag{4}$$

as the associated natural boundary conditions.

It has also been shown [10] that the formulation of (1) corresponds to a positive semidefinite operator—an advantage for the subsequent finite element solution.

Equation (1) is now minimized by the Rayleigh–Ritz procedure combined with the finite element method. Details are given elsewhere [10] and the basic approach follows that of an earlier program description [11]. The unit cell of Fig. 2 is first divided into a patchwork of triangles in the $r-z$ plane. Over every triangle, each field component H_r, H_θ, and H_z is expressed as a complete polynomial in (r, z) with $\exp(j\omega t)\cdot\exp(-jn\theta)\cdot\exp(-j\beta_0 z)$ as an implied multiplying factor. Polynomials of degree one to four are used in any triangle, and the degrees may be the same or different over the many triangles. An advantage of using the same degree everywhere is that the resulting field representation is continuous in r and z everywhere inside the cavities. The permittivity is assumed constant over each triangle, but may vary from triangle to triangle.

Rather than use explicit polynomial coefficients of r and z in each separate triangle, it is more convenient to consider the field components in terms of 'nodal' values. For first degree polynomials, fields are expressed in terms of the three nodal values at the triangle vertices. Second-, third-, and fourth-degree polynomials are similarly expressed in terms of 6, 10, and 15 nodes, a typical arrangement being shown in Fig. 3 for degree 3.

Substituting these piecewise continuous polynomials for H_r, H_θ, and H_z into (1), and partially differentiating with respect to each separate nodal value of H_r, H_θ, and H_z, gives the standard matrix eigenvalue equation

$$\boldsymbol{Q}x = k^2 \boldsymbol{R}\boldsymbol{x} \tag{5}$$

where

$$k^2 = \omega^2 \mu \epsilon \tag{6}$$

and the vector $\boldsymbol{x}$ is given by

$$\boldsymbol{x} = \begin{pmatrix} \boldsymbol{a} \\ \boldsymbol{b} \\ \boldsymbol{c} \end{pmatrix}. \tag{7}$$

The vector $\boldsymbol{a}$ consists of the nodal values of H_r, viz., the unknown values of H_r at all the nodes defined over the unit

TABLE I
DENSITY OF MATRIX Q OF (5) (AND MATRICES R_{ii} OF (5) AND (8),—VIZ. THE PERCENTAGE OF ELEMENTS WHOSE VALUE IS NONZERO

Number of nodes:	30	100	300	1000
Polynomial degree				
1	20	6	2.2	0.7
2	30	10	3.5	1.1
3	40	15	5	1.7
4	60	20	7	2.2

cell—and $\boldsymbol{b}, \boldsymbol{c}$ have similarly the H_θ and H_z nodal values.

$\boldsymbol{Q}$ is complex Hermitian and $\boldsymbol{R}$ is real symmetric, positive definite, arising from the 'inner products' of the numerator and denominator respectively of (1).

Generally, we have

$$\boldsymbol{Q} = \begin{pmatrix} \boldsymbol{Q}_{11} & \boldsymbol{Q}_{12} & \boldsymbol{Q}_{13} \\ \boldsymbol{Q}_{21} & \boldsymbol{Q}_{22} & \boldsymbol{Q}_{23} \\ \boldsymbol{Q}_{31} & \boldsymbol{Q}_{32} & \boldsymbol{Q}_{33} \end{pmatrix} \tag{8}$$

$$\boldsymbol{R} = \begin{pmatrix} \boldsymbol{R}_{11} & 0 & 0 \\ 0 & \boldsymbol{R}_{22} & 0 \\ 0 & 0 & \boldsymbol{R}_{33} \end{pmatrix}. \tag{9}$$

For angular independent modes, the above matrices split up to the separate TM_{0m} modes (involving $\boldsymbol{Q}_{22}$, $\boldsymbol{R}_{22}$, $\boldsymbol{b}$, and hence H_θ) and TE_{0m} modes (involving $\boldsymbol{Q}_{11}$, $\boldsymbol{Q}_{13}$, $\boldsymbol{Q}_{31}$, $\boldsymbol{Q}_{33}$, $\boldsymbol{R}_{11}$, $\boldsymbol{R}_{33}$, $\boldsymbol{a}$, $\boldsymbol{c}$, and hence H_r and H_z).

Detailed development of these matrices is described in the thesis [10], where canonical forms are given for the 'element describing matrices' and assembly of the 'global matrices' [11].

B. Matrix Solution

The theory described so far could be considered a generalization of the earlier TM_{01} work [4], with extensions being to angular dependent modes and to treatment of arbitrary phase-shift per unit cell. A further extension lies in our use of specially developed sparse matrix methods for solving (5). When the cavity section is divided into many triangular elements, the matrix elements of (5) are zero for all pairs of associated nodes that do not belong to the same triangle. This follows because any field component value at a node only contributes to the integrals of (1) via integration over the triangle(s) containing that particular node. Table I shows typical values of the matrix densities, viz., the proportion of matrix elements that are not zero.

Earlier results of our work [12] used standard dense matrix algorithms for the solution of (5), but their use, as in earlier TM_{0m} work [4] is clearly inefficient in computer storage and time when 90 percent or more of the matrix elements are precisely zero. A special algorithm has been developed [10] and, being of general application, is described separately [13]. Briefly, the method combines subspace iteration [14] with linked-index techniques [15] to give any number of selected eigenvalues and, if wanted, the associated eigenvectors. A special feature of the implemented method is that, by taking total advantage of the sparsity of the matrices in (5), the array storage is unusually economical. If, for a given choice of cavity, of general pattern of triangular elements, and of polynomial degree, we simply increase the number of triangular elements, the usual direct matrix methods require an array that is proportional to the square of N, the number of nodal field values (which equals the matrix order). By contrast, with our sparse matrix algorithm, the array is merely proportional to N.

III. RESULTS

The analysis was applied to TM_{0m} modes, both in dielectric-loaded circular waveguide [10] and in dielectric-loaded coaxial cavities of complicated shape for use in dielectric loss measurements [16]. But results will now be given for just two other geometries, both involving comparison with experimental values and with values from other theories. These are the 'iris-loaded waveguide', and an 'arbitrarily shaped linear accelerator cavity'.

As there are no alternative computed results for angular-dependent modes in arbitrary shaped cavities, a particular geometry has been chosen for comparison where the geometry allows a special and accurate theory to be available, together with accurate experimental frequencies [6]. As the earlier work includes a variety of modes, with different values of phase-shift per unit cell, and accuracies generally better than 1 percent (judging from comparison of the earlier theory and experiment), we would regard this as the best independent 'benchmark' for testing of our theory and computer program.

A. An Iris-Loaded Waveguide

An early design of linear accelerator structure uses circular waveguide with periodic loading by a conducting iris, and the simple geometry allowed an accurate theory to be applied and compared with experiment [6]. The geometry and dimensions of the basic cell are shown in Fig. 4, which includes the mesh of triangles used for the finite element analysis. All modes analyzed were with this mesh division, involving 48 nodes, 68 triangular elements, and used first-degree polynomials. As TM, TE, and hybrid modes involve respectively 1, 2, and 3 components of field, the corresponding matrix orders are 48, 96, and 144, and the resulting matrix densities are all 12 percent, resulting in about 24 percent after LU decomposition [10], [14]. Finite element results are compared in Table II with the earlier theoretical and experimental results [6], where the same nomenclature for the hybrid modes has been adopted.

These results were obtained on the minicomputer system GEC 4082/4085 at University College, and accuracy is therefore limited by the core storage restriction of about 160 kbytes for workspace, and by the mantissa of 3 bytes (24 bits). Finite element solutions are known to improve substantially with mantissa length [11], and benchmark tests of our sparse matrix algorithm on a CDC 7600, with 60 bit mantissa, have given excellent results [13].

As expected, accuracy of the finite element results in Table II diminishes with increasing mode number–there

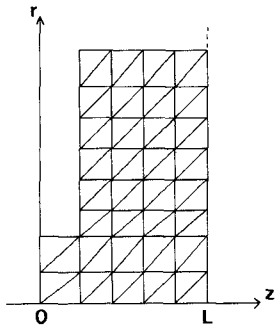

Fig. 4. Unit cell for the iris-loaded waveguide. Dimensions are as in [6], viz guide radius = 41.1 mm, iris hole radius = 10.9 mm, iris thickness = 6.1 mm, and cell length = 26.2 mm.

TABLE II
FREQUENCIES IN MHZ OF 9 MODES IN THE IRIS-LOADED WAVEGUIDE OF FIG. 4

	$\beta_0 L = 0$			$\beta_0 L = \pi/2$			$\beta_0 L = \pi$		
	F.E.	Theor.	Exp.	F.E.	Theor.	Exp.	F.E.	Theor.	Exp.
TM_{01}	2858	2840	2836	2901			3086	2872	2872
E/H_{11}	4456	4385	4376				4442	4266	4250
E/H_{21}	6116	5940	5932	6017			6262	5924	5915
TM_{02}	6685	6551	6550	6852			7227	6722	6741
H/E_{11}	6362	6198		7189	6667	6755	7522	7407	7650
E/H_{12}	8289	8082	8065	8259	7943	8010	8303	7630	7610
H/E_{21}	8083	8203		8198	8218	8495	8487	8232	8440
TM_{03}	8222			8347			8751		
TE_{01}	8793	8632		8858	8639	8284	8426	8646	8244

$\beta_0 L$ gives operation at different phase shifts per unit cell (see Section II). Columns headed 'F.E.' denote results from this finite element theory; other columns give theoretical and experimental values from [6].

being no more than 6 and 9 sampling points in the z and r directions, respectively.

B. A Practical Linear Accelerator Cavity

The ability of the finite element program to deal with cavity sections of arbitrary shape is illustrated in this test. The TM_{01} cavity was designed by Oldfield [17] at the University of Cambridge, for electron-optics research. One quarter of the longitudinal section is shown in Fig. 5, and the finite element triangles used are superimposed together with the degree of polynomial used in each triangle. A mixed order approximation [11] was selected in order to take maximum advantage of the available computer workspace and the computer program's flexibility. A high polynomial degree is advisable in the re-entrant region where the fields vary rapidly, and so a combination of reduced element size and high degree polynomials was used in this region, while in the rest of the structure where weaker fields are expected, larger triangles and lower degrees were adopted.

The lines of constant H_θ calculated from our finite element program are given in Fig. 6.

Experimentally, the TM_{01} mode was used with the central

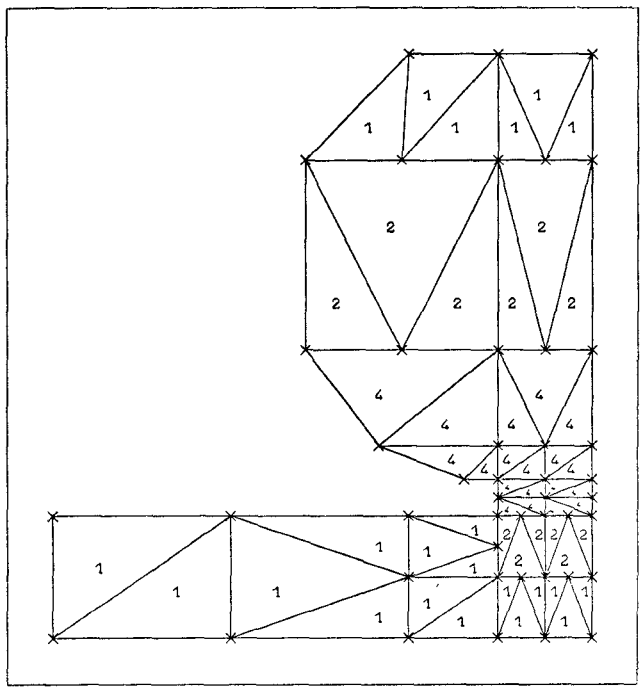

Fig. 5. One quarter of the longitudinal section of the symmetrical cavity.

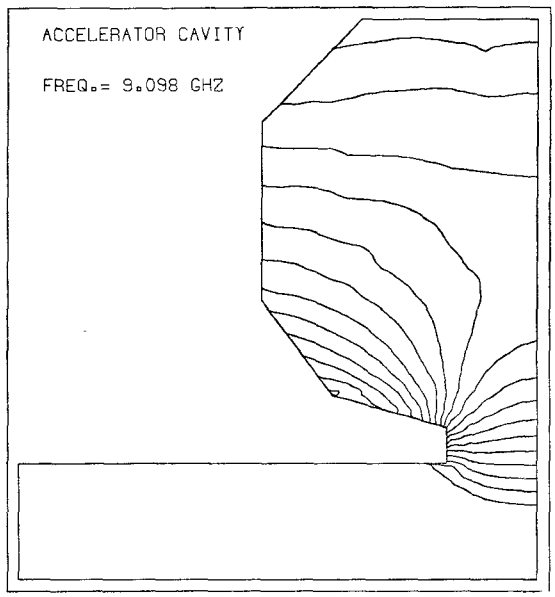

Fig. 6. H_θ-constant lines calculated for the cavity of Fig. 5

section corresponding to a length of circular waveguide operating well beyond cutoff, in order to prevent fields 'spreading' away from the single cavity. The evanescent nature of the fields into the narrow tube can be seen in the figure.

Table III shows results of the TM_{01} resonant frequencies. Both results from the 'F.E. program' use the same sparse matrix package described in this work, the UCL results being obtained with the 53 elements of mixed degree shown in Fig. 5, using a mantissa of 24 bits on the GEC minicomputer already mentioned. The F.E. results from RSRE were obtained using 60 triangles of fourth degree on an ICL 1906S computer, with a mantissa of 48

TABLE III
FREQUENCIES CORRESPONDING TO THE CAVITY OF FIG. 5

	Frequency in GHz	Error in %
F.E. program (UCL)	9.098	2.68
F.E. program (RSRE)	9.0094	1.68
F.D. program (RSRE)	8.991	1.47
Experiment (UCL)	8.8604	

bits. The F.D. program results are from a finite difference solution on a 100-by-100 mesh specially programmed at RSRE [17].

APPENDIX

A. Spurious solutions

As with many finite element and finite difference approaches to field problems, 'spurious solutions' have sometimes emerged from our calculations, viz. solutions that do not correspond to a physical solution. This problem appears to be a 'running sore' in the topic of finite element analysis, and the authors have found no cure, but have investigated some diagnostic tools. Details of our study are given in [10], but a summary is now given.

We firstly observe that *no* spurious solutions were found for angular independent TM modes. They *do* occur for TE and for hybrid modes, and they fall into two fairly clear categories. The first one includes 'modes' with very low eigenvalues, often clustered near zero and separated by some orders of magnitude from the rest of the spectrum. The second group of spurious solutions is found interspersed with the real solutions, with eigenvectors having elements with absolute values similar to the nearest real solution. An analysis of their phases, however, shows a very fast spatial variation usually related to the number of nodal points in the direction concerned.

For the right-hand expression (1) to be zero, we must have

$$\boldsymbol{H} = \nabla\phi \tag{10}$$

where ϕ is arbitrary. The boundary condition of (4) is then identically satisfied by (10). The arbitrariness of ϕ gives an infinite multiplicity of eigenvalue zero to (1), and this is believed to account for the first category of observed spurious solutions. They do not occur for TM modes because the operator of (1) is strictly positive-definite.

The same operator is positive semi-definite for TE and hybrid modes, providing the admissible functions are restricted so as to satisfy (4), but it ceases to be definite if (4) is not forced. Indefinite systems are known to give rise to spurious solutions, and so enforcement of boundary conditions (4) would appear a likely worthwhile scheme.

Konrad [18] suggests that in order to satisfy (4) it is sufficient to make $\boldsymbol{H}$ tangential at the boundary—but we disagree with this. Enforcing

$$\boldsymbol{n}\cdot\boldsymbol{H} = 0 \tag{11}$$

indeed guarantees that

$$\boldsymbol{n}\cdot\nabla\times\boldsymbol{E} = 0 \tag{12}$$

if we define $\boldsymbol{E}$ via

$$\nabla\times\boldsymbol{E} = -j\omega\mu H \tag{13}$$

but this does *not* guarantee the satisfaction of (4). One cannot beg the question that both of Maxwell's curl equations are satisfied—and generally the finite element solution will *not* satisfy Maxwell's equations, having finite polynomial field expansions.

We have, nevertheless, experimented with the numerical enforcement of (11) together with

$$\frac{\partial(\boldsymbol{n}\times\boldsymbol{H})}{\partial\boldsymbol{n}} = 0 \tag{14}$$

at all conducting boundaries. Starting with solutions where (2) is the only forced boundary condition, the spectrum has been obtained when (11) is additionally forced, and when (11) and (14) are added. As each constraint is applied, some spurious solution eigenvalues are indeed eliminated, but not all.

One successful experiment, from the point of recognizing spurious solutions in order to distinguish them from physical modes, was to investigate the divergence of any field solutions. From any eigenvector, an approximate integral of $|\nabla\cdot\boldsymbol{H}|^2$over the cavity is calculated. An exact physical field solution would have zero divergence, and it was found that the calculated integrals were indeed significantly lower for the real solutions, so as to be quite recognizable.

POSTSCRIPT

Following a referee's suggestion, we have added references [19] and [20] that concern the finite element matrices of the type used in this work. The references do not result in complete programs for cavity analysis, nor were they actually used in our work, but they give element matrix details in more generality (and are more accessible) than our earlier references [9], [10].

REFERENCES

[1] W. Walkinshaw, "Theoretical design of linear accelerators for electrons," *Proc. Phys. Soc.*, pp. 246 *et seq.*, 1948.
[2] M. Chodorow *et al.*, "Stanford high-energy linear electron accelerator (Mark III)," *Rev. Sci. Instr.*, vol. 26, pp. 134–204, Feb. 1955.
[3] H. C. Hoyt, "Designing resonant cavities with the LALA computer program," *Proc. Linear Accelerator Conf.*, (Los Alamos), pp. 119–124, Oct. 1966.
[4] A. Konrad, "Linear accelerator cavity field calculation by the finite element method," *IEEE Trans. Nucl. Sci.*, vol. NS-20, pp. 802–808, Feb. 1973.
[5] K. Holbach and R. F. Holsinger, "Superfish–A computer program for evaluation of RF cavities with cylindrical symmetry," *Particle Accelerators*, vol. 7, pp. 213–222, 1976.
[6] J. B. Davies and B. J Goldsmith, "An analysis of general mode propagation and the pulse-shortening phenomenon in electron linear accelerators," Philips Res. Rep., vol 23, pp. 207–232, 1968.
[7] H. Hahn, "Deflecting mode in circular iris-loaded waveguides," *Rev Sci. Instr.*, vol. 34, pp. 1094–1100, Oct. 1963.
[8] R. E. Collin, *Foundation for Microwave Engineering*. New York: McGraw-Hill, 1966.
[9] G. Y. Philippou, "Solution of a circularly symmetric periodic structure by the finite element method," University College London, Dept. Rep. EEE/77/8, Mar. 1977.
[10] F. A. Fernandez, "Finite element analysis of rotationally symmetric

electromagnetic cavities," Ph.D. thesis, Dept. Electronic and Electrical Eng., University College London, Sept. 1981.
[11] A. Konrad and P. Silvester, "Scalar finite element program package for two dimensional field problems," (Program description), *IEEE Trans. Microwave Theory Tech.*, vol. MTT-19, pp. 952–953, Dec. 1971.
[12] G. Y. Philippou, G. S. Gupta, and J. B. Davies, "Finite-element analysis of angularly dependent modes in a general rf periodic cavity," *Electron. Lett.*, vol. 17, pp. 588–589, Aug. 1981.
[13] F. A. Fernandez and J. B. Davies, "Iterative solution of $Ax = \lambda Bx$ for A, B of arbitrary sparsity," submitted for publication, *Int. J. Numer. Meth. Eng.*
[14] K. J. Bathe and E. L. Wilson, "Numerical methods in finite element analysis," New Jersey: Prentice Hall, 1976.
[15] I. S. Duff, "A survey of sparse matrix research," *Proc. IEEE*, vol. 65, pp. 500–535, 1977.
[16] P. Axon, "A radio frequency calorimeter for the measurement of small dielectric absorptions in polymeric materials and its analysis using a computer program," Ph.D. thesis, Dept. Electronic and Electrical Eng., University of College London, June 1980.
[17] L. C. Oldfield, private communication, Royal Signals and Radar Establishment, Malvern, England.
[18] A. Konrad, "Vector variational formulation of electromagnetic fields in anisotropic media," *IEEE Trans. Microwave Theory Tech.*, vol. MTT-24, pp. 553–559, Sept. 1976.
[19] A. Konrad, "High-order triangular finite elements for electromagnetic waves in anisotropic media," *IEEE Trans. Microwave Theory Tech.*, vol. MTT-25, pp. 353–360, 1977.
[20] P. Silvester, "Construction of triangular finite element universal matrices," *Int. J. Numer. Meth. Eng.*, vol. 12, pp. 237–244, 1978.

✤

J. Brian Davies (M'73) was born in Liverpool, England in 1932. From Jesus College, Cambridge, England, he received a degree in mathematics in 1955. From the University of London, England, he received the M.Sc. degree in mathematics, the Ph.D. degree in mathematical physics, and the D.Sc. (Eng.) degree in engineering in 1957, 1960, and 1980, respectively.

From 1955 to 1963 he worked at the Mullard Research laboratories, Salfords, Surrey, England, except for two years spent at University College, London, England. In 1963 he joined the Staff of the Department of Electrical Engineering, University of Sheffield, England. Since 1967 he has been on the Staff at University College, London, where he is Reader in Electrical Engineering. From 1971 to 1972 he was a Visiting Scientist at the National Bureau of Standards, Boulder, CO. His research work has been with problems of electromagnetic theory, especially those requiring computer methods of solution, but recently has extended into field problems in acoustic microscopy.

Dr. Davies is a member of the Institute of Electrical Engineers, London, England.

✤

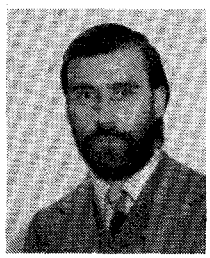

F. Anibal Fernandez was born in Santiago, Chile, in 1945. He received the degree of Ingeniero Matematico in 1973 from the Universidad de Chile, Santiago, where he has been a member of the academic staff of Electrical Engineering since 1969.

From October 1978 to October 1981 he was on leave at University College London, England, where he received his Ph.D. degree in electrical engineering in 1981. His main research interests concern applied electromagnetic field theory, especially those aspects involving numerical techniques.

✤

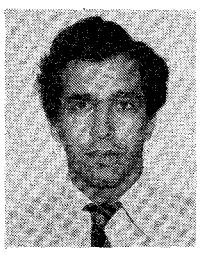

Glafkos Y Philippou (M'81) received the B.Sc. (Eng.) and the Ph.D. degrees in electronic engineering from Queen Mary College, University of London, in 1972 and 1975, respectively.

In 1975 he joined the Electrical and Electronic Engineering Department of University College, University of London, as a Research Assistant. He worked mainly on the application of the finite element technique to the solution of electromagnetic problems. In 1977 he joined the RF Technology Centre at ERA Technology Ltd., in Leatherhead, Surrey, England, where he was primarily involved in the theoretical studies of electromagnetic problems. His current interests are in the application of the finite element technique to the problem of scattering from finite objects.